An Energy-Efficient Analog-to-Pulse Encoding for Short-Range High-Density Wireless Telemetry

Mohammad R. Haider, Adam Farr, Showmik Singha, and Syed K. Islam
Department of Electrical Engineering and Computer Science
University of Missouri
Columbia, MO, U.S.A.
{mhaider, islams@missouri.edu}

***Abstract*—The prevalence of sensors and sensor networks has resulted in the Internet of Things (IoT), transforming modern lifestyles. However, resource-constrained IoT edge devices require inventive sensing, computing, and wireless telemetry strategies to support the massive number of devices in an IoT network. Traditional telemetry and data encoding schemes for short-range sensor networks are limited by network bandwidth, data processing capability, and power constraints imposed by the battery energy density. To mitigate these challenges, an energy-efficient architecture is presented for analog orthogonal pulse (AOP) generation and AOP-based data encoding for high-density spectrum-efficient wireless telemetry. Unlike conventional digital pulse-based encoding, higher-order analog orthogonal pulses are used for spectrum-efficient data encoding. The orthogonal pulse generator contained a reduced number of functional blocks for energy efficiency. The MATLAB-Simulink package is used to design and simulate the proposed encoding architecture and, finally, embedded into a microcontroller unit. Test results show the successful generation of analog orthogonal pulses and pulse-based signal encoding.**

***Index Terms*—analog orthogonal pulse, data telemetry, internet-of-things, pulse encoding,**

I. Introduction

With the ever increasing trend of micro- and nano-devices, and wireless technology, we are entering an era of internet-connected devices—the Internet of Things (IoT)—which is reshaping both our lifestyles and work environments [1], [2]. These devices range from simple in-home temperature sensors to sophisticated brain-machine interfaces for prosthetic limbs [3], [4]. They are continuously collecting data and influencing everyday activities, advanced healthcare, industrial automation, transportation, etc. It has been predicted that by 2027, over 41.0 billion IoT devices will be connected to existing networks, collecting data on our daily activities, work routines, movements, and the maintenance of essential machinery. The increasing prevalence of edge devices demands innovative sensing, computing, and communication strategies with key design features including but not limited to energy efficiency, distributed processing, security, wireless connectivity, and more.

The incorporation of numerous recording channels within a confined space and wireless data acquisition have become achievable in these days. However, this expansion of recording channels gives rise to a significant surge in data volume, presenting a considerable hurdle for wireless data transmissions. For instance, a recording system with 128 channels and 8-bit resolution, operating at the Nyquist sampling rate, necessitates a data rate of 20 Mb/s for a 10 kHz target signal [5]. With an escalation in the number of channels, the data rate can elevate to 100 Mb/s or even higher [6]. Supporting such a huge data volume in real-time fashion mandates increased device memory, processing speed, network bandwidth, etc. which are scarce in resource-constrained IoT devices [7], [8].

In the recent years various modulation techniques have been developed to cater to high-density IoT devices, Index Modulation (IM) using orthogonal pulses standing out as a promising method to meet the demands of high-volume data transmission in next-generation IoT networks [9]–[13]. IM techniques hinge on either physical resources, such as antennas and frequency sub-carriers, or virtual building blocks like signal constellation, antenna activation order, and space-time matrix [14]. However, most of the mathematical functions for the design of orthogonal pulses such as the Haar Function [15], the Modified Hermite Polynomial Function (MHP) [16], [17], and the Prolate Spheroidal Wave Function (PSWF) [18], etc. involve complicated math model and power hungry hardware implementation [19]. On the contrary, MHP pulses have lower computational complexity than the PSWF based pulses, and possess the orthogonality properties of nearly constant pulse widths irrespective of the pulse orders. Nevertheless, the conventional MHP generation schemes require the second order derivative and the squared time function, t^2, that complicate the pulse generator's architecture.

In this paper, an analog orthogonal pulse (AOP) generation and pulse based encoding have been discussed. An energy-efficient AOP generator architecture is presented to support high-density data telemetry without requiring extended network bandwidth. MATLAB-Simulink package is utilized to design and simulate the algorithm. Simulation results verify the successful AOP generation, data encoding, and spectrum-efficient high density data communication.

The organization of the paper is as follows. Section II presents the proposed analog-to-pulse encoding architecture, section III shows the simulation and test results, and finally, section IV draws the conclusion.

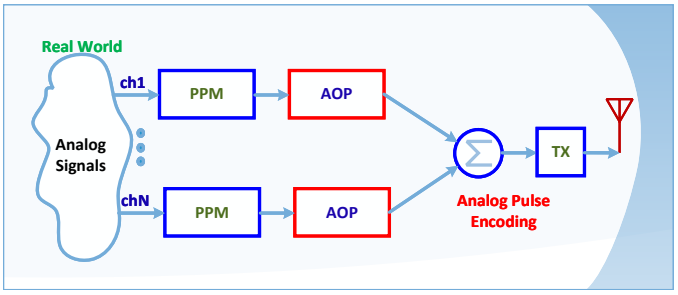

Fig. 1. Schematic diagram of the proposed analog to pulse encoding system consisting of analog orthogonal pulse (AOP) generator block and pulse position modulator (PPM) block.

II. The Proposed Analog-to-Pulse Encoding Architecture

The proposed analog-to-pulse encoding (A2PEn) architecture for an N-channel system is shown in Fig. 1. The A2PEn architecture consists of an analog orthogonal pulse (AOP) generator and a pulse position modulator (PPM) block. Each channel is assigned a distinct order AOP and the channel outputs are combined for simultaneous high-density data transmission. The functional details of the AOP and PPM blocks are presented in the following subsections.

A. Energy-Efficient Analog Orthogonal Pulse Generation

This section demonstrates the development of a mathematical model for analog orthogonal pulse generation. Unlike existing schemes for orthogonal pulse generation, the developed mathematical model offers less number of required functional blocks, reduced system complexity, and enhanced power-efficiency. To overcome the limitations of existing orthogonal analog pulse generation schemes, we propose an innovative choice by following the neuronal coupled first order ionic dynamics to break down the second order system as a combination of two first order systems and sub-GHz operation to reduce the system complexity and power consumption of the orthogonal pulse generation.

The analog orthogonal pulse generation architectures as reported in [16], [17] incorporate second order derivative and t^2 function resulting in 5 integrators, 8 multipliers and 5 adders to generate two different order MHPs, implying a high power dissipation for system implementations. To reduce the computational burden of the pulse generator, an innovative modification is reported in [20] and the modified equations can be written as

$$\tau \dot{h}_n(t) = -\frac{t}{2\tau} h_n(t) + n h_{n-1}(t) \tag{1}$$

$$\tau \dot{h}_{n-1}(t) = \frac{t}{2\tau} h_{n-1}(t) - h_n(t). \tag{2}$$

Unlike previous architectures, (1) and (2) imply two interdependent dynamic systems with more computationally-efficient architecture to generate two MHPs simultaneously.

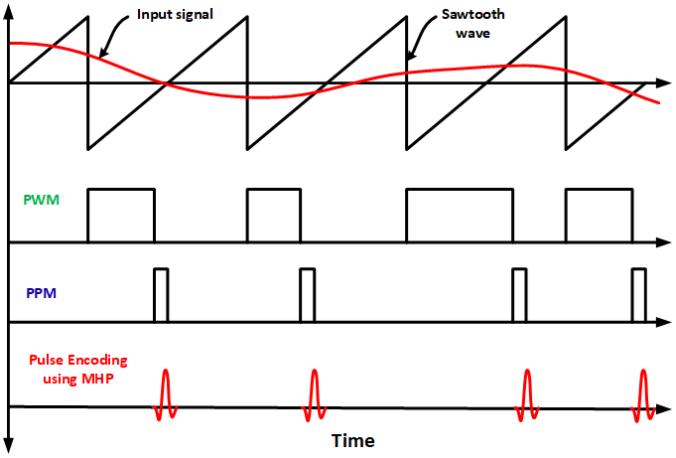

Fig. 2. Schematic diagram of analog input signal to pulse width modulation (PWM) and pulse position modulation (PPM) waveform generations. The sawtooth waveform is for comparing the input signal with a predefined threshold.

B. Pulse Position Modulator

This section discusses analog orthogonal pulse based pulse position modulation (PPM) scheme. Unlike traditional rectangular pulse based PPM, analog orthogonal pulses are used that enables simultaneous sampling and transmission of multichannel data without requiring complex hardware architecture or extended network bandwidth.

PPM is usually used in digital communication system by varying the position of pulses. Instead of using the amplitude, frequency, or phase of a carrier signal, the PPM focuses on the timing of individual pulses to encode the input signal.

Owing to its simplicity in architecture and resilience to amplitude variation, the PPM finds applications in power-constrained low-to-moderate data rate systems. However, the conventional PPM scheme suffers from low data rate due to the requirement of precise timing synchronization at the receiver ends. To overcome the limitation of low data rate, analog orthogonal pulse index based encoding scheme is proposed in this work. The proposed scheme encodes the signal by transforming the analog input signal to time delayed orthogonal pulse index generation. The time delay between two successive pulse indexes represents the change in input signal amplitude.

The functional block diagram of the PPM is shown in as a sub-block in Fig. 3. The PPM sub-block takes the analog input signal and compares it with the ramp signal of a sawtooth wave. The frequency of the sawtooth wave is selected carefully so that multiple signal comparison or the Nyquist rate sampling of the input signal is satisfied. The comparator output generates pulse width modulated pulses which are then passed through another comparator block and the output of the comparator triggers a monostable flip-flop to generate the PPM pulses. The PPM pulses are utilized to reset the integrator blocks of the AOP generator sub-block and triggers the generation of a new analog orthogonal MHP pulse.

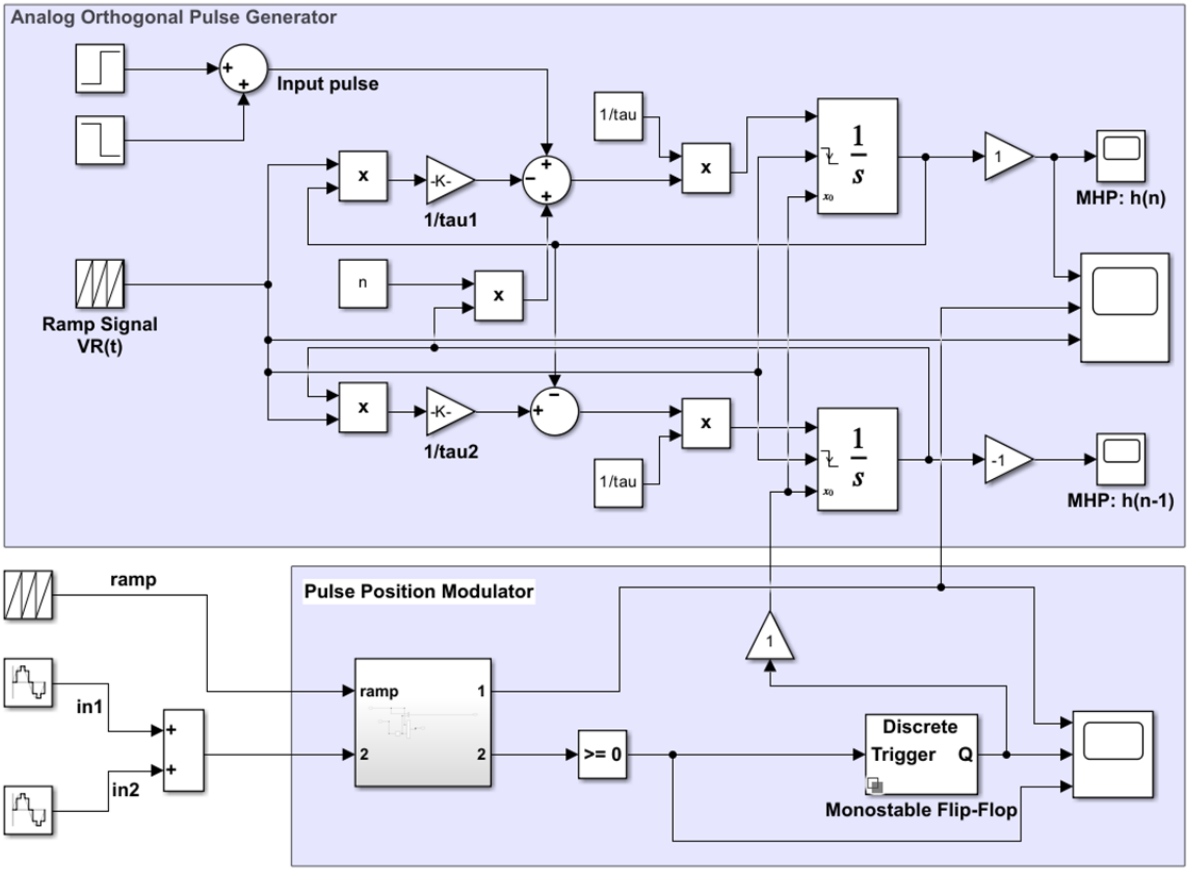

Fig. 3. The schematic block diagram of the proposed energy-efficient analog to pulse encoding system. At the core of the system, there is a modified hermite polynomial based analog orthogonal pulse generator block. The analog input signal is sampled by a ramp signal and a short duration one-shot pulse is generated by the pulse position modulator block to initiate the analog orthogonal pulse generation. An external trigger pulse is used with the integrator blocks to reset the integrators and enable periodic operation of the analog orthogonal pulse generator. A normalization block is utilized to scale the diminishing amplitudes of the higher order analog orthogonal pulses.

III. Simulation and Test Results

The design and simulation of the AOP and pulse encoding schemes are done using MATLAB-Simulink package.

A. Analog Orthogonal Pulse Generation

The proposed architecture manifesting (1) and (2) is implemented in MATLAB-Simulink as shown in Fig. 3 and the simplified model contains only 2 integrators, 5 multipliers, and 3 adders in the system. A time-scale factor of 1×10^{-9} and a gain value of $tau = 150 \times 10^{-6}$ are selected to produce ~200 us pulse width. In Fig. 3, all the tau values are identical, i.e., $tau = tau1 = tau2$. Considering the small pulse expansions caused by the higher order, we have assigned a time-window of 200 us. For a 200 us time-window, a ramp signal, $V_R(t)$, from -50 mV to 50 mV is used to represent the time function $\frac{t}{2}$ and generate the MHP pulses. By setting different integer values to n, the two interdependent dynamic systems can generate n^{th} and $(n-1)^{th}$ order MHPs.

B. Analog Orthogonal Pulse Encoding

The analog orthogonal pulse encoding scheme employs a PPM block and the time delay of the generated PPM pulses

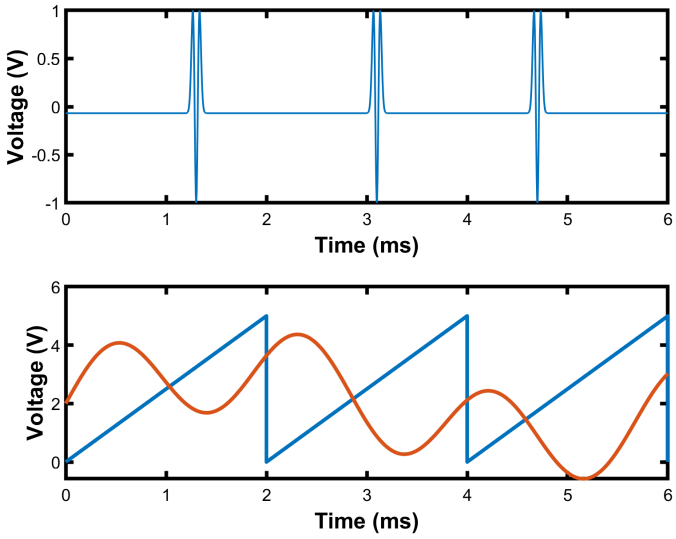

Fig. 4. Simulation results showing an unknown analog input signal sampled by a ramp signal (bottom plot) and the generation of pulse position analog orthogonal pulse (upper plot) at the cross-over or sampling-point between the analog input and the ramp signals. A second order (n = 2) analog orthogonal pulse is generated at the sampling-point.

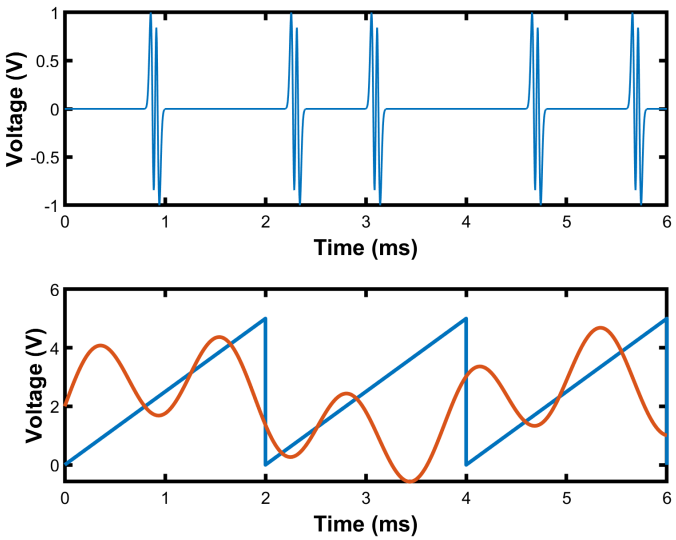

Fig. 5. Simulation results showing an unknown analog input signal sampled by a ramp signal (bottom plot) and the generation of pulse position analog orthogonal pulse (upper plot) at the cross-over or sampling-point between the analog input and the ramp signals. A third order (n = 3) analog orthogonal pulse is generated at the sampling-point.

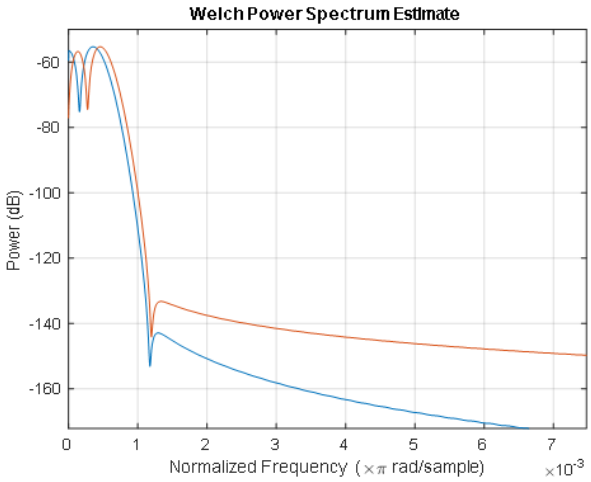

Fig. 6. Power spectra of two distinct order (2^{nd} and 3^{rd}) MHP based AOPs. It can be seen that both the spectra are occupying almost identical spectral bandwidth.

indicate the amplitude change of the analog input signal. The PPM pulses are then used as triggers to generate the AOP. Fig. 3 shows the entire analog orthogonal pulse encoding scheme.

A sawtooth wave signal is used to sample the analog input signal. The input signal is compared with the ramp of the sawtooth signal and as the input signal exceeds the ramp signal, an AOP is generated. The frequency of the sawtooth signal is selected $4\times$ of the Nyquist sampling rate for ease of reconstruction at the receiver unit. The reconstruction unit is not explained here for the brevity of the paper.

Fig. 4 shows an unknown analog input signal is being sampled by a ramp signal. As the input signal crosses the ramp signal, a distinct AOP is generated. For Fig. 4 a second order AOP is generated at the sampling-point. For multiple

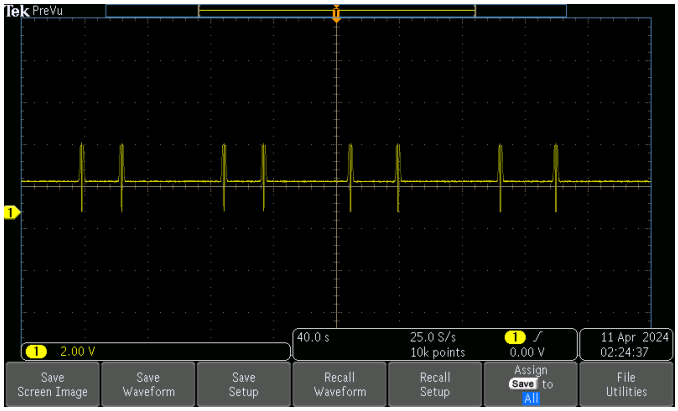

Fig. 7. Screenshot from oscilloscope showing microcontroller generated 2^{nd} order MHP based AOPs.

channels, a distinct order MHP based AOP is assigned as an identifier for each channel and as a result the generated distinct AOPs from different channels do not interfere with each other. The orthogonality property of different order MHP based AOP allows coexistence of multiple channels and data without requiring extended bandwidth or time multiplexing.

Fig. 5 depicts the similar phenomena of sampling of an unknown analog input signal by a ramp signal; however, a third order (n = 3) analog orthogonal pulse is used to encode the input signal. Similar to Fig. 4, the relative time difference of the AOPs indicate the relative difference in amplitude of the unknown input signal. By using distinct order AOPs for encoding different analog input channels, the generated AOPs can be superimposed to generate a composite pulse without destroying the individual AOP signal properties, thanks to the orthogonality properties of the MHP based AOPs. Fig.

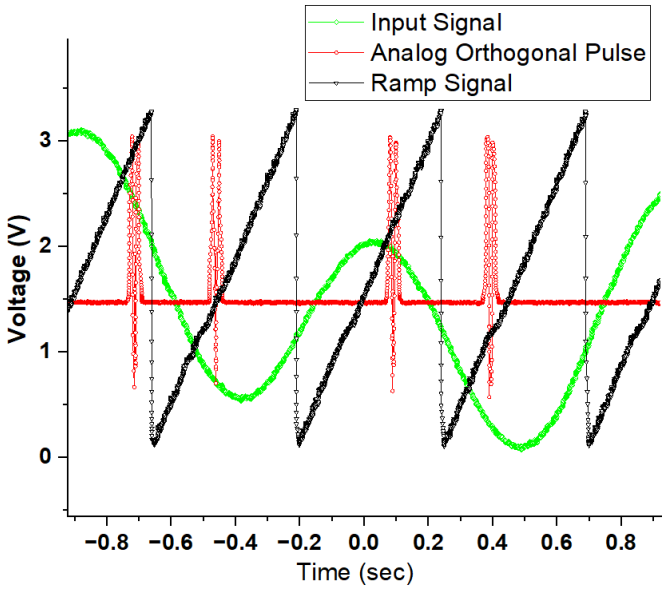

Fig. 8. Test results of different signals from the microcontroller board using experimentally extracted datasets. The microcontroller generated signals successfully recreates the proposed analog-to-pulse encoding scheme.

6 shows the power spectra of two distinct order MHP based AOPs, where it can be seen both power spectra are occupying the same bandwidth, i.e., no additional bandwidth requirement is needed to transmit these two AOPs. Another advantage of using MHP based AOPs is their almost constant bandwidth or time duration that enables simpler design of correlation based receiver for detecting the AOPs from the incoming composite pulses. Unlike traditional rectangular pulse based PPM signals, the proposed scheme can accommodate $n\times$ channels or data within the same bandwidth, highlighting the efficacy of the proposed scheme.

After successful MATLAB-Simulink simulation, the proposed analog-to-pulse encoding algorithm was programmed to a microcontroller board and the output signals are viewed using oscilloscope in a laboratory test setup. For the test and validation of the proposed algorithm, an Arduino Nano33 board is utilized because of its analog output capability. However, due to the hardware limitation of the Arduino Nano33 board, a 200 ms AOP is used instead of 200 us AOP. The analog input signal was generated internally to the microcontroller board and sampled using a ramp signal. Fig. 7 shows the screenshot from oscilloscope for the generated 2^{nd} order MHP based AOPs. Due to only one analog output pin of the Arduino Nano33 board, all the signals were viewed sequentially and stored the data from oscilloscope to a corresponding Excel file. All the experimentally extracted data are combined and plotted using Origin software. Fig. 8 depicts the plots of different signals from the experimentally extracted data sets. As is evident from Fig. 8, the microcontroller generated signals successfully recreate the analog-to-pulse encoding scheme.

IV. Conclusion

This work presents an efficient analog orthogonal pulse based encoding scheme for spectrum-efficient telemetry for resource-constrained IoT edge devices. Unlike traditional rectangular pulse based pulse position modulation, distinct order analog orthogonal pulses are utilized to encode the analog input signals. The generated AOPs are then superimposed for spectrum-efficient simultaneous transmission of multichannel signals using the same network bandwidth. A modified hermite polynomial based AOP generation scheme is utilized with reduced number of functional blocks to enable higher energy efficiency. The proposed analog-to-pulse encoding scheme is simulated using MATLAB-Simulink and later on embedded on to a microcontroller platform. Both simulation and experimental results demonstrate the efficacy of the proposed architecture. In future, a transmitter block will be integrated with the microcontroller unit to demonstrate spectrum-efficient high density wireless data telemetry.

Acknowledgment

This work was supported by the National Science Foundation (NSF), USA under Award nos. ECCS-1813949 and ECCS-2201447. However, any findings, comments, and suggestions expressed herein are those of the authors and do not necessarily reflect the views of NSF.

References

[1] David, "Wearable iot devices: applications and potential risks," may 25, 2024. [Online]. Available: https://www.deepseadev.com/en/blog/wearables-and-iot/

[2] S. Mukhopadhyay, N. Suryadevara, and A. Nag, "Wearable sensors and systems in the iot," *Sensors*, vol. 21, no. 23, p. 7880, 2021. [Online]. Available: https://dx.doi.org/10.3390/s21237880

[3] M. A. Lebedev and M. A. Nicolelis, "Brain-machine interfaces: past, present and future," *Trends Neurosci*, vol. 29, no. 9, pp. 536–46, 2006.

[4] M. A. Lebedev, A. J. Tate, T. L. Hanson, Z. Li, J. E. O'Doherty, J. A. Winans, P. J. Ifft, K. Z. Zhuang, N. A. Fitzsimmons, D. A. Schwarz, A. M. Fuller, J. H. An, and M. A. L. Nicolelis, "Future developments in brain-machine interface research," *Clinics*, vol. 66, pp. 25–32, 2011.

[5] M.-S. Chae, Z. Yang, M. Yuce, L. Hoang, and W. Liu, "A 128-channel 6 mw wireless neural recording ic with spike feature extraction and uwb transmitter," *Neural Systems and Rehabilitation Engineering, IEEE Transactions on*, vol. 17, no. 4, pp. 312–321, 2009.

[6] M. Yuce, H. C. Keong, and M. S. Chae, "Wideband communication for implantable and wearable systems," *Microwave Theory and Techniques, IEEE Transactions on*, vol. 57, no. 10, pp. 2597–2604, 2009.

[7] T. Noguchi, M. Nakagawa, M. Yoshida, and A. G. Ramonet, "A secure secret key-sharing system for resource-constrained iot devices using mqtt," in *2022 24th International Conference on Advanced Communication Technology (ICACT)*, 2022, pp. 147–153.

[8] F. Pereira, R. Correia, P. Pinho, S. I. Lopes, and N. B. Carvalho, "Challenges in resource-constrained iot devices: Energy and communication as critical success factors for future iot deployment," *Sensors*, vol. 20, no. 22, 2020. [Online]. Available: https://www.mdpi.com/1424-8220/20/22/6420

[9] M. K. Hossain and M. R. Haider, "Analog pulse based data transmission for internet-of-things applications," in *2020 11th International Conference on Electrical and Computer Engineering (ICECE)*, 2020, pp. 53–56.

[10] M. K. Hossain, Y. Massoud, and M. R. Haider, "A spectrum-efficient data modulation scheme for internet-of-things applications," in *2020 IEEE 63rd International Midwest Symposium on Circuits and Systems (MWSCAS)*, 2020, pp. 770–773.

[11] M. K. Hossain and M. R. Haider, "Channel decoding using cyclic elimination algorithm for pulse based uwb transceiver," in *2020 11th International Conference on Electrical and Computer Engineering (ICECE)*, 2020, pp. 85–88.

[12] M. K. Hossain, M. M. Rana, and M. R. Haider, "Spectrum-efficient analog pulse index modulation for high-volume wireless data telemetry," *IEEE Internet of Things Journal*, vol. 10, no. 11, pp. 9556–9564, 2023.

[13] M. K. Hossain and M. R. Haider, "A multi-bit data modulation using orthogonal pulses for high-density data transmission," in *2021 IEEE International Midwest Symposium on Circuits and Systems (MWSCAS)*, 2021, pp. 599–602.

[14] X. Cheng, M. Zhang, M. Wen, and L. Yang, "Index modulation for 5g: Striving to do more with less," *IEEE Wireless Communications*, vol. 25, no. 2, pp. 126–132, 2018.

[15] L. Zhang and Z. Zhou, "Research on orthogonal wavelet synthesized uwb waveform signal," in *IEEE International Symposium on Communications and Information Technology, 2005. ISCIT 2005.*, vol. 2, 2005, pp. 830–832.

[16] M. Ghavami, L. B. Michael, S. Haruyama, and R. Kohno, "A novel uwb pulse shape modulation system," *Wireless Personal Communications*, vol. 23, no. 1, pp. 105–120, 2002.

[17] L. Michael, M. Ghavami, and R. Kohno, "Multiple pulse generator for ultra-wideband communication using hermite polynomial based orthogonal pulses," in *Ultra Wideband Systems and Technologies, 2002. Digest of Papers. 2002 IEEE Conference on*, 2002, pp. 47–51.

[18] R. Dilmaghani, M. Ghavami, and A. Aghvami, "Uwb multiple-pulse generator and transmitter," in *Ultra Wideband Systems, 2004. Joint with Conference on Ultrawideband Systems and Technologies. Joint UWBST IWUWBS. 2004 International Workshop on*, 2004, pp. 117–121.

[19] B. Allen, S. Ghorashi, and M. Ghavarm, "A review of pulse design for impulse radio," in *Ultra Wideband Communications Technologies and System Design, 2004. IEE Seminar on*, 2004, pp. 93–97.

[20] Y.-G. Li, M. R. Haider, and Y. Massoud, "An efficient orthogonal pulse set generator for high-speed sub-ghz uwb communications," in *2014 IEEE International Symposium on Circuits and Systems (ISCAS)*, 2014, pp. 1913–1916.